AD-A068 918 DELAWARE UNIV NEWARK INST OF ENERGY CONVERSION F/G 9/3
SOLAR ONE: FIRST RESULTS. PART 5: THE SOLAR-ELECTRICAL SYSTEM,(U)
1975 D B MILLER, H M WINDAWI, K W BOEER N00014-71-C-0169

UNCLASSIFIED NL

1 OF 1
AD A068918

END
DATE FILMED
7-79
DDC

LEVEL II

2

Contract N00014-71-C-0169
(15)

(6) Solar One: First Results.

Part 5: The Solar-Electrical System

by

(10) D. B. Miller**, H. M. Windawi and K. W. Boer

Institute of Energy Conversion, University of Delaware

Newark, Delaware 19711

411 147

(12) 41 pp

(11) 1975

Abstract

A The photovoltaic conversion subsystem including electrical energy storage and power processing is described. It is shown that CdS/Cu_2S solar cell arrays are useful to produce a significant fraction of the electrical energy needs of a single family dwelling and, when properly deployed and loaded, show promise for an attractive life expectancy.

NR-372-053

Date: 1975

* Partially sponsored by a group of Electric Power Utilities, NSF/RANN, ONR and NASA.

** On leave from the School of Electrical Engineering, Purdue University, W. Lafayette, Indiana.

411 147

1. Introduction

The solar-electrical system of Solar One consists of CdS/Cu_2S solar cell panels connected to an electrical power processing and storage subsystem. These solar cell panels are deployed in the roof collectors of Solar One.

Since only a limited quantity of such CdS/Cu_2S cells was available, only three of the 24 roof collectors are filled with solar cells, containing a total of 936 individual cells. This is a large enough number to perform a statistical analysis, hence no attempts were made in the first phase of experimentation to increase the number of solar cell panels.

In order to simulate occupation of the entire roof with solar cells, a controlled power supply was employed, slaved to the present solar cell panels and amplifying the harvested electrical energy with the proper amplification factor.

The system permits studies of its electrical performance characteristics specific to the behavior of the solar cells and their connection to a set of lead acid batteris. Special attention is given to obtaining actual harvesting amounts and to accumulation of life expectancy data.

2. Experimental System

2.1 The Solar-Electric System

The solar-electric system is diagrammed in Figure 1. Note that it is a three-wire, +120 V/0V/-120 V d-c system with a solar

electric source*, a series circuit of batteries, controls and d-c loads in parallel across each 120V side of the system. A transfer switch also allows the d-c loads to be energized from the a-c Newark Municipal utility supply. Some details of each element of this experimental system are given in the following sections.

2.2 The Solar Cell Array

CdS/Cu_2S photovoltaic cells are used in Solar One to convert the sun's radiant energy directly into electricity. These cells, which have been described in the literature (1, 2), are in the form of a multiple layer "sandwich" as shown in Figure 2; photovoltaic conversion occurs due to photoelectron action near the heterojunction between the copper sulfide and cadmium sulfide layers. Each cell has approximately 3" X 3" surface area; the voltage-current curves shown in Figure 3 typify the range of cells deployed in two subpanels on the roof of Solar One.

These solar cells are arranged in nine sets of 104, connected in series, and mounted in a 46 inch by 31 inch "subpanel" (13 columns with eight cells per column) as shown in Figure 4. Figure 5 shows voltage-current characterisitics of two of the 104-cell subpanels. The similarity to the single cell curve (Figure 3) is evident, but a substantial loss in current and voltage and

---

*With solar cell panels presently only in one of the two branches and two auxiliary controlled amplifiers to simulate complete roof coverage.

some rounding of the curves are observed. This is due to cell mismatch, some cell shorting during installation, transmission loss through two protective glazing layers, and elevated temperature.

The first two reasons for lower power output are avoidable with a larger sample of cells for selection and with experience for proper panel fabrication. Transmission losses are estimated to reduce* the current output by 14%, the voltage is estimated to be reduced* by 14% when the panel operates at 150°F.

One uses four subpanels connected in series to provide 120 volts, which is near the maximum power point for the four-subpanel circuit. This four-subpanel series group is connected to one branch of the ± 120V system. With better cell matching, only 3.7 subpanels, i.e. 385 cells @0.31 volts (see Section 2.3), are expected to deliver 120 V at maximum power.

Since the electrical behavior of a well matched high efficiency panel is similar to a lower efficiency panel, i.e. the output of the lower efficiency panel is reduced by an essentially constant factor for different light intensities and temperatures, it seems to be justified to evaluate the Solar One performance in the following respects:

A. Performance as if all collectors were filled with subpanels having the same characteristics as the series connection of four subpanels (1-1, 1-2, 2-1 and 2-3) now in use (i.e. including mismatch).

---

*compared to the air mass 1, 25°C values.

B. Performance as if all collectors were filled with the best subpanel (2-1) currently deployed on Solar One (i.e. all subpanels perfectly matched).

C. Performance as if all collectors were filled with the best cell currently deployed on Solar One.

D. Performance as if all collectors were filled with 8% cells.

The above cases can be simulated with a photovoltaic amplifier as described in Section 2.3.

Oxygen, water vapor and high temperature have deteriorating effects on the CdS/Cu_2S solar cells (see Section 3) and special precautions must be taken if long life is desired. The sketches of the subpanels in Figure 4 show that the cells are kept within a hermatically sealed enclosure, with a variety of gaskets and sealants now being tested. A continuous flow of "high purity dry" nitrogen at a positive pressure is maintained through each subpanel to insure that air and water vapor are kept out. The back sides of the cell mounting plates are finned for cooling purposes. Three subpanels are then mounted in each of three of the standard thermal panels on the Solar One roof and the air stream flowing through the panel collects heat from the solar cell subpanels and simultaneously keeps the cells from reaching excessive temperatures.

2.3 Photovoltaic Amplifier

A photovoltaic amplifier was built to provide electric energy proportioned to the energy harvested from one or

several subpanels as described in Section 2.2, and to simulate total roof deployment.

The photovoltaic current amplifiers are Sorensen Model DCR150-15A (150V, 15A) power supplies which have both voltage and current control and limit circuits. They have been modified so that their output currents are real-time-slaved to the actual current output of the solar panel circuit as delivered to a set of lead acid batteries. A block diagram of this solar current amplifier subsystem is shown in Figure 1. The amplification ratio can be set at any desired value (up to the maximum power rating of the amplifier) and is calculated with respect to surface ratio of total panels to actual cell array surface and to its efficiency ratio as explained below (see also Section 2.2, cases A-D).

As described in Section 2.2, four subpanels are linked in series to achieve the nominal 120V level at which most residential loads operate. A series connection of the four subpanels 1-1, 1-2, 2-1 and 2-3 in fact delivers maximum power at 120V when the solar radiation level is $85mW/cm^2$. This maximum power is substantially below the sum of maximum power values of each subpanel for reasons of panel mismatch.

The solar cell circuit is connected directly to a set of 10 batteries hence providing some voltage stabilization. However, the line voltage varies slightly and is determined by the state of charge of the batteries and whether the batteries at any moment are being charged or discharged. The actual voltage might therefore range between 140V, when the batteries are near full charge

and are being charged, down to 105V when the batteries are being discharged at their lower operable charge state. At these extremes, the power being delivered by the solar cell array at 85mW/cm^2 is within 10% of the maximum power value.

Each subpanel has 104 solar cells, each cell having an active area of 54.76 cm^2. For separation between rows of cells, a 1 mm gap is required, adding 0.75 cm^2 of area to each cell.* Hence, the total area required to produce the present operating voltage is 104 X 55.51 cm^2 = 5773.04 cm^2. Four such subpanels (4 X 104 = 416 cells) then require 4 X 5773.04 cm^2 = 23092.16 cm^2. When properly encapsulated into 4 X 8 foot frames (27534 cm^2), such an array would fill 0.839 of one panel. A 3 cm wide empty strip close to the edge of the 4 X 8 foot frame has been included to prevent excessive cell shadowing during early morning and late afternoon hours.** Since there are 24 available 4 X 8 foot panels on the roof, we arrive at an amplification factor of 24/.839 = 28.6 for Case A (Section 2.2).

In order to calculate the amplification factor for Case B of Section 2.2, the reduction of power output due to panel mismatch had to be taken into consideration. This is done by determining the ratio of the current at the maximum power point of sub-

---

*Currently there is an additional "dead" area of approximately 3.5 cm^2 between each cell where the cells are interconnected. This area is eliminated in cells now being produced, using a special interconnect method.

**The voltage-current operating point of such a shadowed cell drops and allows that cell to be overheated by the current driven through it by the other unshadowed cells in the series circuit.

panel 1-2 (see Figure 5) to the obtained current of the series of subpanels while connected to the batteries. This ratio does vary with the battery voltage (charging or discharging mode) and values between 1.6 and 2.4 are obtained for the subpanel series 1-1, 1-2, 2-1, 2-3. For practical purposes it may suffice to assume a constant value of 2 to yield an average performance. This results in an amplification factor of 57 for case B (Section 2.2).

If we take the best presently deployed cell with its current-voltage characteristic measured in the solar simulator at AM1 and 25°C, as shown in Figure 3, we obtain 0.36 volt for its maximum power point. At 150°F the voltage is reduced by approximately 50mV, resulting in 385 solar cells needed to produce the required battery charging voltage, or a correction factor of 416/386 = 1.08 compared to case B. Moreover, the current output of the cell (0.68 amp) is higher by a factor of 1.15 compared to the measured output of the panel 1-2 (0.42 X 100/85 X 1/0.86 = 0.51 amp)*. The calculated ratio for case C in Section 2.2, therefore, is 68. Finally, for case D only the efficiency ratio of the best presently deployed cell $\frac{0.68A \times 0.36V}{54.76\ cm^2} / 100\ mW/cm^2 = 4.47\%$ to the expected 8% cell is used, yielding a ratio of 122.

Table 1 gives the current amplification ratios as calculated above.

---

*Calculated at 100mW/cm^2 and without double glazing (1/0.86) to compare with the cell tester results of the best cell.

2.4 Batteries

A set of twenty, 12-volt automobile-type, lead-acid batteries presently used at Solar One, are installed in two series circuits, thereby yielding +120/0/-120V (Figure 1). These are rated at approximately 90 A-Hr (20 Hr rate), so the total energy storage is about 19 kWh. ESB, Inc., donated these units and has replaced them with forty 6V higher capacity (200 A-Hr), longer-life "electric vehicle" batteries which will be installed after the present set is adequately tested.

During periods of solar harvesting, the solar panels are directly connected to the set of batteries. Although this mode of operation is relatively primitive, as it does not take into consideration differences in cell output at different illumination, it is a mode far superior to a constant resistive load operation. This can be seen by comparing curves 1 and 2 in Figure 6 taken at different illuminations. Using the same resistive load R_{mp} tailored for the maximum power point at full illumination (a), even at half illumination the obtained power (b) is already far from the new maximum power point. Using a battery-regulated voltage, however, the power output (c) is much closer to the maximum point. Moreover, since a lower illumination will also result in a lower panel temperature with increased open circuit voltage (curve 3), the actual power output (d) will be even closer to the maximum power point.

This fact permits using a very simple solar panel/battery circuit without much loss in the total energy output of the solar conversion unit and could considerably reduce first costs.

2.5 Loads

Solar One is outfitted with the loads found in a typical house, including lights, refrigerator, range, washer and drier, and wall outlets for small appliances, clocks, radios, TV, etc. Presently, until dc-to-ac inverters are installed, only the lights are used in solar-electric system testing. In addition, high-power, variable rheostats are employed for a controlled load simulation. Currently these rheostats can be operated by hand following a prescribed load program.

As a research laboratory, Solar One has additional electric needs, most of which are supplied through separate circuits and are metered separately. Since it also houses a solar exhibition located in the garage and is open on parts of two days to the general public, still additional electric energy needs are supplied and separately metered.

It is therefore advantageous to simulate the entire load by using the rheostats and using load profiles as they are experienced in typical single family homes of comparative size. The actual profiles used in these Solar One experiments are based on information supplied by the Delmarva Power & Light Co., obtained from other private and government sponsored studies and publications, and extracted from some actual data recorded at a residence.

A fixed load, equivalent to the average daily residence value, is often adequate for many tests and was also used occasionally.

2.6. Utility Electric Power

One of the main restraints of solar houses will be that it is an economic disadvantage to make these houses independent from utility power. This is caused by the fact that sunlight is available only intermittently (day/night cycle and cloud cover) and that energy storage is expensive*. One must therefore attempt to use a large fraction of the energy directly while it is supplied from the solar conversion source, and have major fractions of sequences of cloudy days covered by power from utilities.

For the home owner, then, energy storage has the useful functions to regulate operation at or near maximum power point and to bridge and level transients, such as caused by starting motors or by fast moving clouds. For the power utility, energy storage can be used as an instrument for load management and particularly for load leveling. Thus, it is a significant advantage for the home owner and for the power utility involved, to operate the solar house system in conjunction with the utility grid. Continued testing of the Solar One electrical system should provide data on which this cooperative operation concept can be quantitatively evaluated.

For purposes of obtaining proper information on electric energy needs of the solar thermal part of the system, a variety of watt-hour meters measures the flow of electric energy to the different fans and auxiliary heaters (see Part 2 of this publication).

---

* To bridge extensive periods of inclement weather would require excessive storage never used to full capacity (safety factor).

2.7 Controls

Voltage-sensitive controls are built into the electrical system (Figure 1) in order that automatic cycling of the battery subsystem can take place. These controls cause the ac/dc transfer switch to move to the ac position when the battery voltage drops below a given present level (e.g. $\pm$105V) and simultaneously begin charging the batteries from the utility supply. When battery voltage then reaches a present high level, indicating sufficient charge, the system is returned to the dc mode. These controls can be overridden when charging through the solar subsystem takes place. In actual operation the charging from utility supply for test purposes will be eliminated.

2.8 Instrumentation

Digital meters, with calibrated shunts and voltage dividers are used to measure voltage and current of the solar array, current amplifier, battery and load branches. Chart recorders give simultaneous continuous records of up to three channels. A precision power supply is incorporated as a part of the system for regular calibration and testing.

A multiplexer is being prepared so that all electrical signal channels can be monitored on a single chart record. The desirability of converting all information to digital form is being evaluated.

Temperature data are measured by the multipoint recorders which are used regularly for evaluation of thermal collectors.

3. First Experimental Results

3.1. Solar Cell Performance at Roof Top Conditions

The compatibility of the CdS/Cu_2S solar cell for use on a large terrestrial scale is governed to a great extent by its stability under varied conditions of electrical loading, temperatures and ambient gases.

For the conversion of solar radiation to electrical energy, the cells are electrically loaded. Improper loading, however, causes a "load degradation": if the load is such that the voltage across the cell is greater than .39 V (e.g. open circuit voltage) the copper sulfide may decompose and copper is released which shorts out the cell. Generally, however, the voltage at the maximum power point is less than .39 V especially when the temperature is higher than 25°C. Hence, when the cell (or array) is kept close to the maximum power point, no degradation should result from this mode. New results on cell development show that this mode is avoidable (3).

The effect of elevated temperatures on the photovoltaic characteristics of the cells is enhanced degradation. High temperature enhances the diffusion of copper ions from the Cu_2S into the CdS (4, 5). The resulting copper doping in CdS may affect the diode characteristics through the changes in the potential distribution near the heterojunction, causing changes in the leakage current. Moreover, small changes in the stoichiometry of the Cu_2S near the junction may result in changes of the collection efficiency (short circuit current). Phase changes in the Cu_2S may accompany the changes in temperature (above about 160°F) (6). While the phase changes are

reversible, the changes caused by diffusion are not; hence, the temperature should be kept low to obtain maximum life expectancy and higher output.

Panels exposed to rooftop conditions in which the temperature was allowed to rise to stagnation levels ($\gtrsim$ 200°F) show considerable degradation (Fig. 7)*. Although the cells are encapsulated (Figure 2) the encapsulation is somewhat permeable to oxygen and water vapor which usually leaks through the encapsulation. When this occurs, it has been found that the degrading effects of water vapor (7) and air (8) are drastic**(Figure 8)*. Reaction of these gases with the surface of the Cu_2S is accelerated by illumination. Surface reaction, if limited to a few layers on the surface, may increase surface recombination of electrons and holes generated by photon absorption. Thicker layers may decrease the electron-hole generation rate and increase the recombination rate. Even the build-up of a layer of different chemical composition near the surface, creating another junction, is possible. One can only speculate on some of the mechanisms at the present time. It has been shown, however, that the use of high purity dry nitrogen gas does indeed prevent such drastic degradations.

Thus, oxygen, water vapor and high temperature have deteriorating effects on the CdS/Cu_2S solar cells, and the encapsulating procedures described in Section 2.2 are desired. A flushing with "high purity dry" nitrogen is provided to counteract possible small

---

* In test panels deployed on the roof of the Institute of Energy Conversion.

** Significant recovery of this kind of degradation is observed after treatment in H_2 at elevated temperatures.

leaks and always provide positive inside panel pressure, preventing back diffusion of air into the panels.

Figure 9 shows the development of the efficiency* of sub-panel 1-2 during the period from October 1973 to June 1974. It seems that within the span of time the yield went through a seasonal cycle where the lowest efficiency was obtained during the winter months. No noticeable overall degradation can be detected during the ten-month period shown.

The seasonal behavior of the efficiency may be explained by one or all of the following factors:

1. Seasonal variations in the spectral distribution of the solar radiation, while not measured, may be significant. Spectral responses of the cells vary from cell to cell. Hence the output of the cells varies according to the spectral distribution.
2. A mismatch in the output of cells connected in a panel would vary according to the spectral distribution of solar radiation.
3. Since the panels are located on the roof of Solar One, where the roof is elevated at about 45° from the horizontal and at about south-north direction, the normal solar radiation falls approximately parallel to the normal to the plane of the panels during the months of October and March while making angles of $\sim$ 18° during January and 28° during July at solar noon (9). Reflection of the radiation from the glazing of the panel is the least at normal incidence so that less actual radiation is collected by the cells during December than that which is collected by the Pyroheliometer (where the protecting glass is hemispherical) to which calibration is made. Hence the decrease in the measured efficiency.

---

* The efficiency is obtained by dividing the measured power at the maximum power point by the insolation measured with the Epply Pyroheliometer (W/cm^2) multiplied with the total area of the solar cells

4. Other factors that should be considered are the diffuse and horizontal components of solar radiation.

Slight variations in temperature of the panel do not account for such changes since they are measured and appropriate corrections are made.

It may be concluded that deployment of Cu_2S/CdS solar cells on rooftop conditions, if properly encapsulated, protected from excessive temperatures ($<150°F$) and electrically loaded (< 0.39 volt per cell), can have a long lifetime for photovoltaic conversion. While no estimate can be made for the lifetime based on the results shown, it may be consistent with a predicted value* of more than 20 years when the temperature is maintained below 50°C (8).

3.2. Temperature Stabilization of Subpanels

The temperature of the CdS/Cu_2S cells was controlled by aircooling from the back, using fins to increase heat transfer. From July, 1973 to March, 1974 only 6 fins (3" wide) per panel were used. A flow rate of 225 cfm was employed. With an estimated heat transfer coefficient of 4 $Btu/ft^2hr°F$ (related to projected surface) and heat rate of 300 Btu/ft^2-hr one expects the solar cells to be 75°F above the temperature of the cooling air.

Currently the subpanels used in the electrical system are located at the lower 1/3 and 2/3 position of panels 1 and 3 (see Figure 5 of part 2 of this publication). The maximum air temperature at the upper edge of these positions are 11 and 22°F respectively above inlet temperature at 225 cfm and 300 Btu/ft^2 insolation. With an inlet temperature of 90°F the upper cells would be heated to 185°F, too high for long life expectancy of the CdS/Cu_2S cells.

* Using diffusion data of Cu in CdS

The highest measured values during clear summer noon in 1973 were 180°F in fair agreement with the given estimate.

In March, 1974 new fins were installed as shown in Fig. 4, increasing the estimated heat transfer coefficient to 12 Btu/ft^{2}hr°F, hence reducing under otherwise same conditions the temperature difference between solar cells and cooling air to 25°F. With an inlet temperature of 90°F one expects a maximum cell temperature of 137°F, well within the limits given by enhanced degradation.

Actual values are within experimental errors of the above estimates.

For reasons of saving electrical energy the Solar fan* was off as long as the temperature of the cells did not exceed a certain preset value, e.g. 150°F. At somewhat lower insolation even free convection (chimney effect) was sufficient for proper cooling as shown in Table 2.

It can be expected that improved finning may provide sufficient cooling effect that even during clear summer noon hours very little forced air is necessary to keep the cells below 150°F.

3.3. Electrical System Test Results

Electrical system testing has primarily focussed on a series of day-long duration tests to reveal total system performance characteristics under actual operating conditions. The results of three such tests (January 8, 1974, May 1, 1974 and May 13, 1974) are presented in Figures 10 and 11 and in Tables 3 and 4. The first two days were clear, and the third was partly cloudy. The first

---

* Used to remove heat from the backside of the solar panels.

test (1/8/74) was made before several shorts in subpanel 2-1 were removed; hence the operation was performed with a significantly weaker solar cell array than for the two later tests.

A number of operating characteristics can be identified from these tests:

1. The load is automatically shared between the solar source and the battery; as the solar radiation increases (as in the morning on 1/8/74 and 5/1/74 and intermittently throughout 5/13/74), the load receives more power from the solar cells and less from the batteries, and when solar radiation diminishes, the load is maintained by energy stored in the batteries. This is simply a consequence of the parallel circuit being used and depends merely on slight shifts in voltage level rather than on special control components.

2. As a consequence of item 1 above, however, slight shifts in voltage do occur (see particularly Table 4) amounting to perhaps 5% during the daytime operation.

3. If one is willing to tolerate considerably larger voltage drop and deeper battery cycling, the load can be continued on the d-c system well into the evening.

4. Table 3, summarizing the results of these three tests, shows that a significant percentage of a typical residence's daily base load could be delivered by completely outfitting the Solar One roof with the best present subpanel.

5. Solar-electric conversion efficiency improved a great deal between 1/8/74 and 5/1/74. This is primarily due to elimination of grounds which shorted out a number of cells in one subpanel. Also, the importance of matching the solar cell array to the load and

4. Conclusions and Recommendations - Electrical System

Overall solar-electric system operation has been demonstrated by a series of day-long tests. Total d-c energy delivered to the load has been typical of the daily electric energy consumed by a residence, and a sizable fraction of this energy has come from the amplified solar-electric source. The importance of the battery for voltage regulation, energy storage and maximum power tracking have been shown.

Several recommendations for continued study can be made based on experience gained in these tests:

1. It is known from individual cell tests that all employed cells have better than 3.5% maximum efficiency, but the systems tests show overall efficiency of about 1.6 - 1.8% at best. The major factor in this loss in efficiency is the mismatch among cells in the series array circuit, and we must therefore emphasize the importance of selecting cells which have nearly identical maximum power points.

2. The application of batteries in solar-electric systems needs considerable further evaluation. The economic tradeoffs of light-cycling ("float") vs. deep-cycling (off peak charging and energy storage) must be considered. The optimum voltage at which to operate a "string" of batteries has not been specifically determined, but it probably is more nearly 60V than 120V; this could best be implemented in conjunction with complete inversion to ac.

3. Faster data acquisition and digital data analysis have been found to be necessary for thorough understanding of system performance, particularly during partly cloudy days (such as on 5/13/74) when the system condition is changing rapidly. Transient response of the battery/solar-array source and of residential loads should be determined.

battery voltage is emphasized so that all cells are operated as near to their maximum power point as possible. Due to this mismatch the overall efficiency (∿ 1.5%) is considerably lower than the average efficiency of the cells used (4%).

6. Efficiency is generally lower in the early morning and late afternoon hours as the insolation characteristics cause the cells to be operating off their maximum power points.

7. During the major part of the day, independent of solar radiation conditions, the batteries hold the solar array near the same power efficiency point (see Table 4).

8. The slight fall off in efficiency at midday and in the afternoon is probably due to the increased cell temperature at these times (Figure 11).

A total of ten such full-day, carefully instrumented tests have been performed to date, and one of the important objectives of these tests has been to observe battery operation under deep cycling conditions. Table 5 presents the results of this aspect of these tests, which were consecutively taken without additional charges or discharges. Note that an overall charge/discharge efficiency of 71% has been experienced with no particular care being taken to control or minimize charging energy. It is clear that much better than 71% performance can be obtained if considerable care and control are exercised on the charge cycle. These tests are not adequate, however, to show change in efficiency with life or with depth of cycle, two important characteristics which must be established for future system definition.

5. Acknowledgements

Mr. K. V. Jarva and Mr. R. F. Wieland contributed significantly to the design, fabrication and testing of the electrical system and its various components. Mr. Allan Tyler of the Delmarva Power & Light Co. and Mr. Kevin O'Connor, Program Manager of the Solar One program made many helpful suggestions during the course of this work. The contribution of the batteries by ESB, Inc. has been greatly appreciated. The support of the seven power utilities mentioned in Part 1 and of the University of Delaware is acknowledged.

References

(1) F. A. Shirland, The History, Design, Fabrication and Performance of CdS Thin Film Solar Cells, Advanced Energy Conversion 6, pp. 201-222 (1966).

(2) K. W. Böer, et al, Recent Results in the Development of CdS/Cu_2S Thin Film Solar Cells, 10th Photovoltaic Specialists Conference Record, IEEE, pp. 77-84 (1973).

(3) K. Bogus, et al, Fourth Closing Report, General Electric Company, AEG-Telefunken, Heilbronn (1973).

(4) G. A. Sullivan, Phys. Rev. 184, 796 (1969).

(5) W. Palz, et al, 8th Photovoltaic Specialists Conference Record, IEEE (1970).

(6) W. R. Cook, Jr., The Copper-Sulfur Phase Diagram," Ph.D. Thesis, Case Western Reserve University (1971).

(7) A.E. Spakowski et al, NASA TN D-3663 (1966)

(8) L. Partain and M. Sayed TR No. NSF/RANN/SE/GI-34872/TR73/8.

(9) J. L. Threlkeld, Thermal Environmental Engineering, 2nd Edition, Prentice-Hall, Inc., New Jersey, pp. 279 (1970).

Table Captions

Table 1

Amplification Ratios

Case	Description	Approximate Amplification Ratio
A	Present performance, all roof panels filled	30
B	Best present subpanel, all roof panels filled	55
C	Best present cell, all roof panels filled	70
D	All roof panels filled with 8% solar cells	120

Table 2

Mode	Air temperature In	Air temperature Out	Airflow (cfm)	Insolation W/ft^2	Maximum solar cell temperature	Fan duty cycle
Chimney	88°F	125°F	40	65	149°F	-
Chimney	100°F	130°F	50	40	145°F	-
Forced	73°F	107°F	250	80	130°F	50%

Table 3 Energy Values for Three Tests

(Values apply to the entire system, including both "A" and "B" sides of the $\pm$120V circuit)

Date of Test	1/8/74	5/1/74	5/13/74
Type of Day	clear	clear	partly cloudy
Duration of Test	11h05m	15h22m	11h20m
Energy from solar array	.075 kWh	.20 kWh	.15 kWh
Amplification Factor(≈case B)	48*	59	54
Energy from solar amplifiers	3.51 kWh	11.9 kWh	7.95 kWh
Energy from batteries	10.4 kWh	16.2 kWh	14.9 kWh
Total energy to load	14.0 kWh	28.3 kWh	23.0 kWh
Percent of Load from Amplified Solar Source	26%	43%	35%
Expected solar contribution for case D (ampl. factor 120)	> 65%*	87%	78%

---

* Shorts contained in subpanel 2-1 reduced the output markedly below the base value used for calculation of the amplification factor. Hence substantially more than 65% contribution is expected.

Table 4 Actual Test Data - SOLAR ONE; data taken on 5/13/74; only the "A" Half of the +120V/0V/-120V system is shown.

Time	Voltage	Instantaneous Insolation	Solar Array Power	Solar Amp. Power	Battery Power	Solar Array Efficiency	Comment
	V	w/ft^2	W	W	W	%	
1012	124	-	-	-	920	-	Begin test
1036	123	25	9.3	350	550	1.5	
1045	126	76	32	900	6	1.7	
1115	123	22	8.6	340	560	1.6	
1200	127	95	41	1100	-190	1.7	variable cloud cover
1245	123	20	8.4	280	600	1.7	
1300	128	90	36	1000	-80	1.6	
1345	128	100	41	1100	-200	1.7	
1403	124	42	15	490	390	1.4	
1530	123	35	15	450	470	1.8	
1611	124	69	25	690	190	1.5	
1700	122	47	9.3	350	530	.8	
1800	120	24	3.4	200	1100	.6	load increased
2000	112	-	-	-	1050	-	
2100	107	-	-	-	1040	-	
2130	105	-	-	-	717	-	end of test

Table 5 Battery Cycle Data

Test Date	Beginning Open Current Voltage		Terminal Operating Voltage		Charge Energy to Batteries from Utility (before test)	Discharge Energy from Batteries to Load
	A	B	A	B	kWh	kWh
1/8/74	130	130	115	113	19.3	10.4
1/15/74	128	129	105	105	16.5	14.5
1/24/74	128	129	117	112	20.5	10.5
1/29/74	129	130	105	107	14.2	15.3
2/6/74	129	129	105	108	17.4	12.6
2/14/74	128	129	105	105	14.7	12.6
2/21/74	127	128	105	105	17.3	13.0
4/2/74	124	126	105	105	15.9	11.1
5/1/74	127	127	105	105	27.7	16.2
5/13/74	127	128	105	105	20.0	14.9
Total					183.5	131.1

Overall Efficiency: 71%

FIGURE LEGEND

1. Block diagram of the solar-electric system.
2. A cross-section of a CdS/Cu_2S solar cell (not to scale) with approximate dimensions of layers.
3. Current voltage characteristics of best and worst cells on Subpanels 1-1 and 1-2, measured in cell tester, AM1 at 20°C.
4. Solar-electric subpanel designs (all four corners sealed with DC3140 or DC3145).
4. (continued) Solar-electric subpanel construction.
5. Current-voltage characteristic of the total Subpanels 1-1 and 1-2 (roof deployment)
   Cell temperatures were in the approximate range 115°F - 130°F.
6. Maximum power points and loading at different temperatures and light intensities.
7. Load voltage of solar roof panel as a function of time with cells encapsulated and kept in dry N_2 but near "stagnation temperatures" (>200°F).
8. Load voltage of solar roof panel as a function of time with cells exposed to humid air.
9. Variations in the efficiency of P1-2 with time.
10. Actual test data - SOLAR ONE; data taken on 1/8/74; only one-half (the "A" side)of the +120V/0V/-120V system is shown.
11. Actual test data - SOLAR ONE; data taken on 5/1/74; only one-half (the "A" side) of the +120V/0V/-120V system is shown.

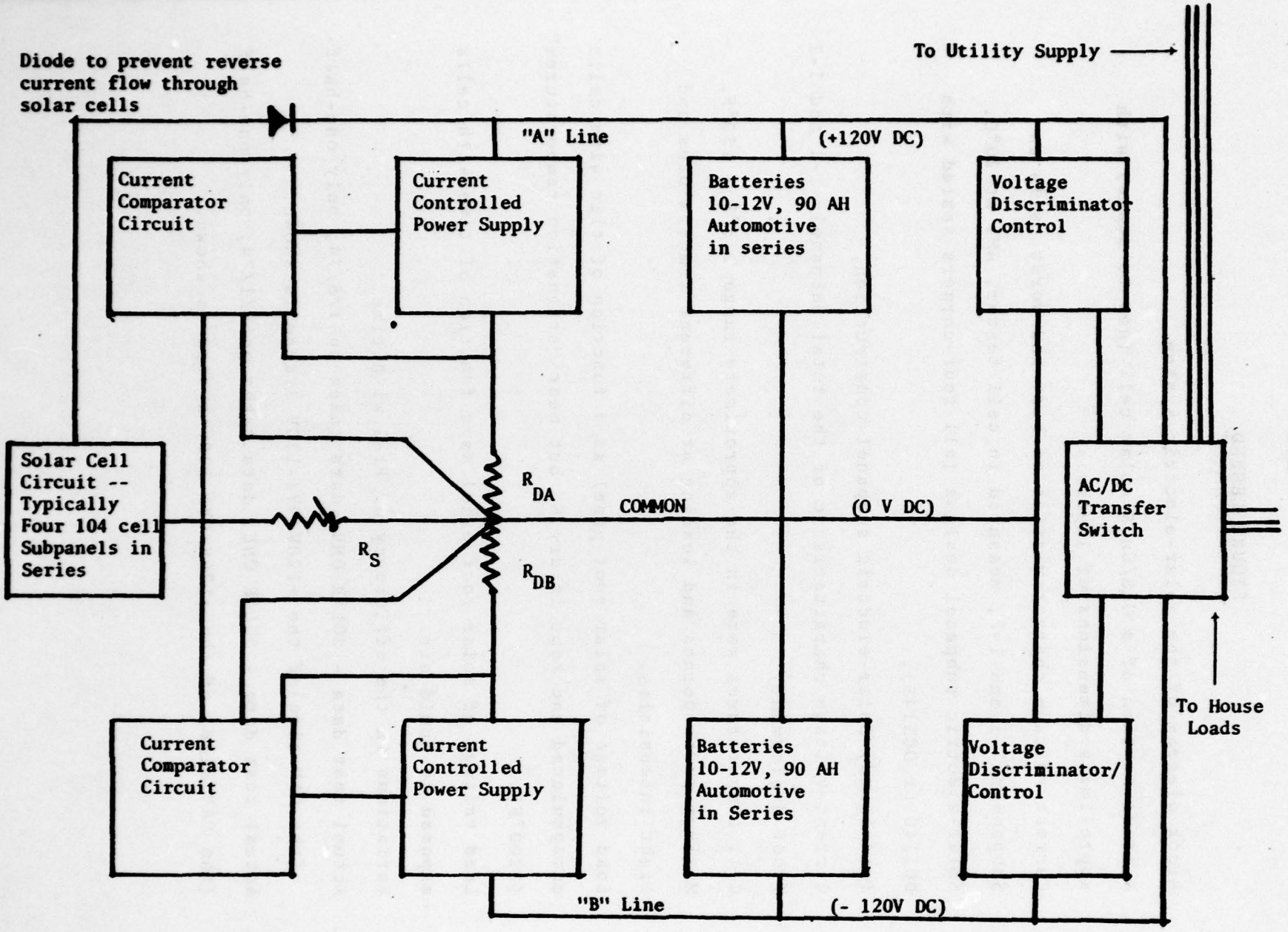
Diode to prevent reverse current flow through solar cells
To Utility Supply
"A" Line
(+120V DC)
Current Comparator Circuit
Current Controlled Power Supply
Batteries 10-12V, 90 AH Automotive in series
Voltage Discriminator Control
Solar Cell Circuit -- Typically Four 104 cell Subpanels in Series
R_{DA}
R_S
R_{DB}
COMMON
(0 V DC)
AC/DC Transfer Switch
To House Loads
Current Comparator Circuit
Current Controlled Power Supply
Batteries 10-12V, 90 AH Automotive in Series
Voltage Discriminator/ Control
"B" Line
(- 120V DC)

FIGURE 1

FIGURE 2

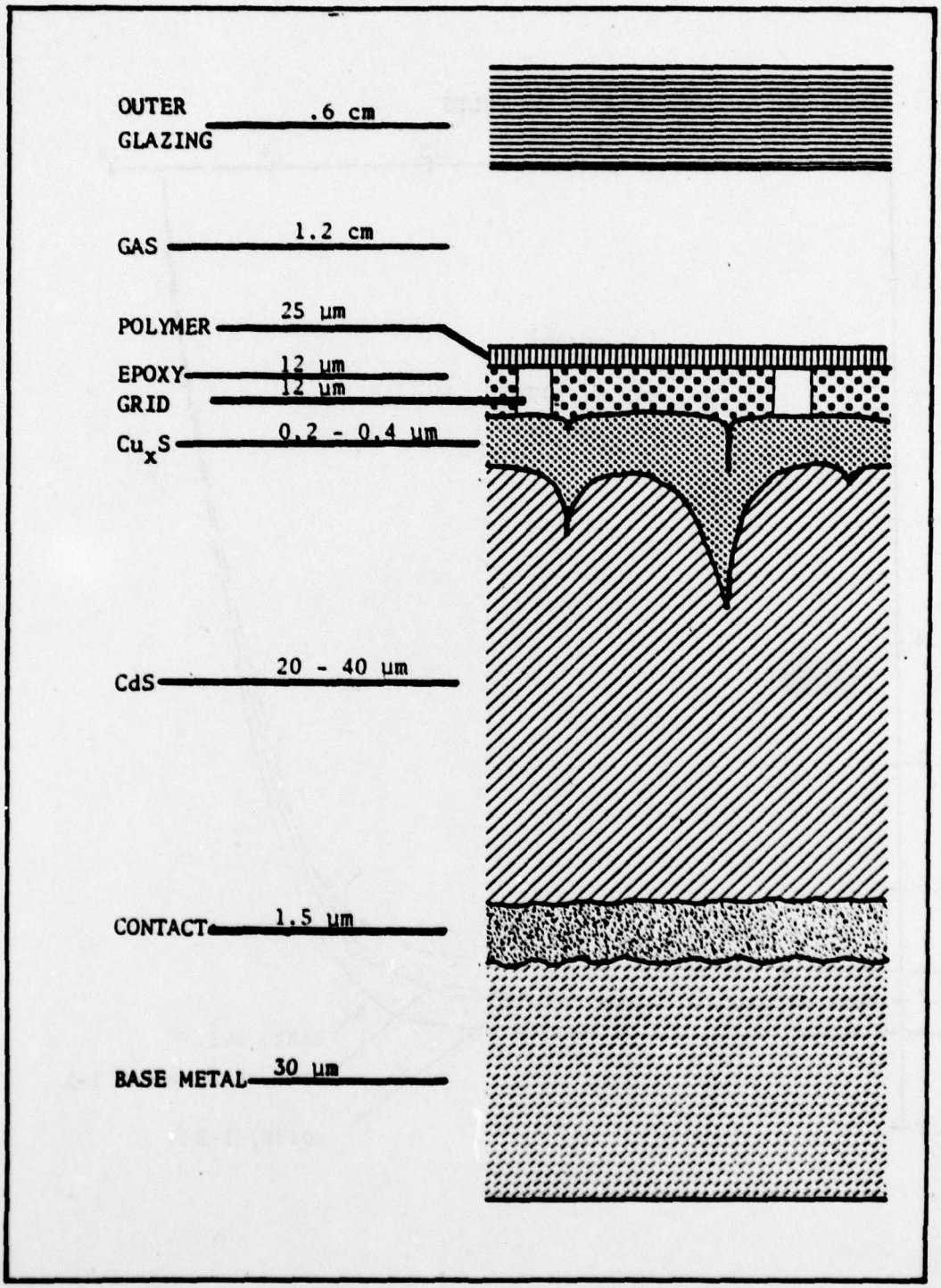
OUTER GLAZING
.6 cm
GAS
1.2 cm
POLYMER
25 µm
EPOXY
12 µm
GRID
12 µm
Cu_xS
0.2 - 0.4 µm
CdS
20 - 40 µm
CONTACT
1.5 µm
BASE METAL
30 µm

FIGURE 3

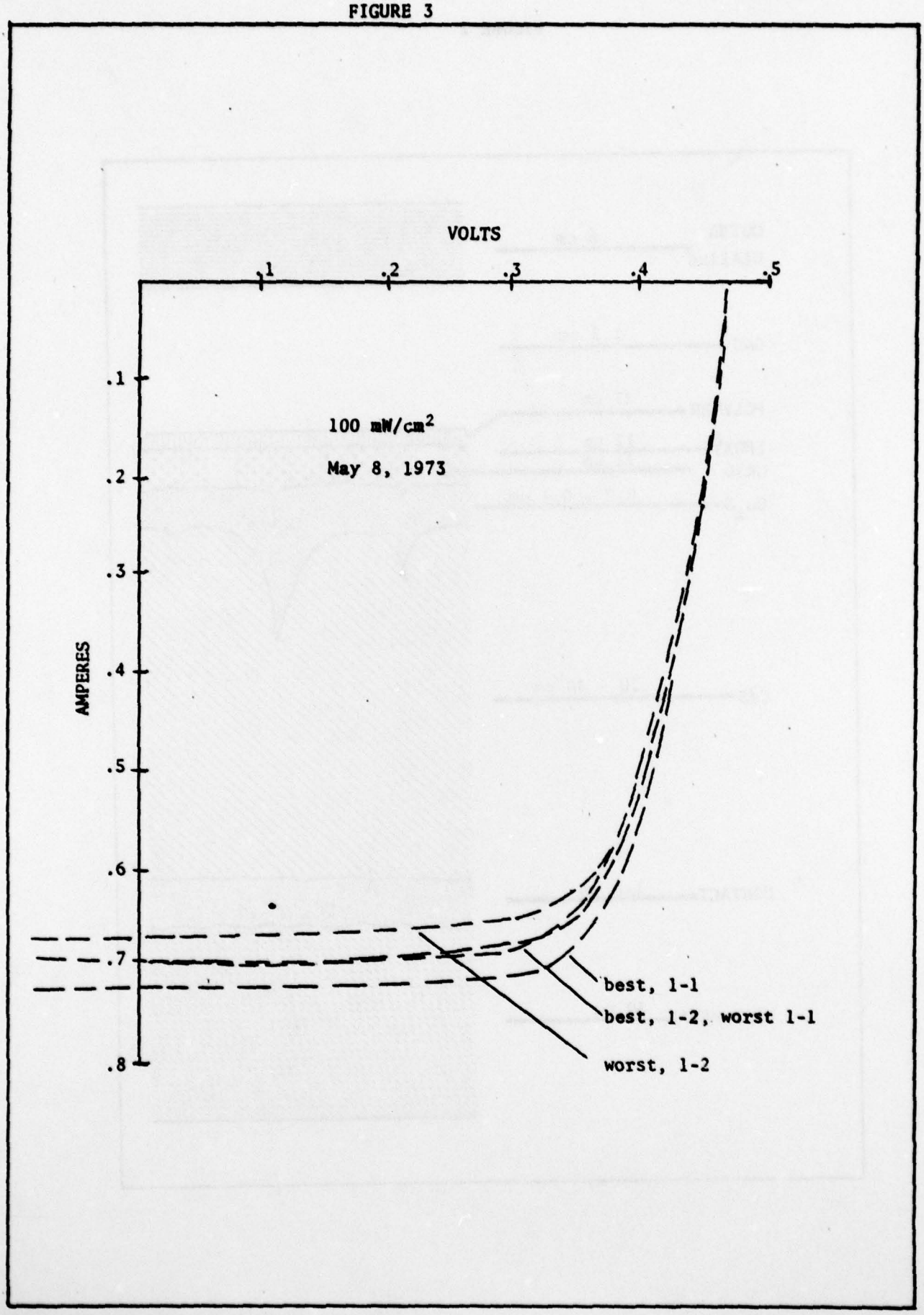
VOLTS
.1
.2
.3
.4
.5
AMPERES
.1
.2
.3
.4
.5
.6
.7
.8
100 mW/cm²
May 8, 1973
best, 1-1
best, 1-2, worst 1-1
worst, 1-2

FIGURE 4

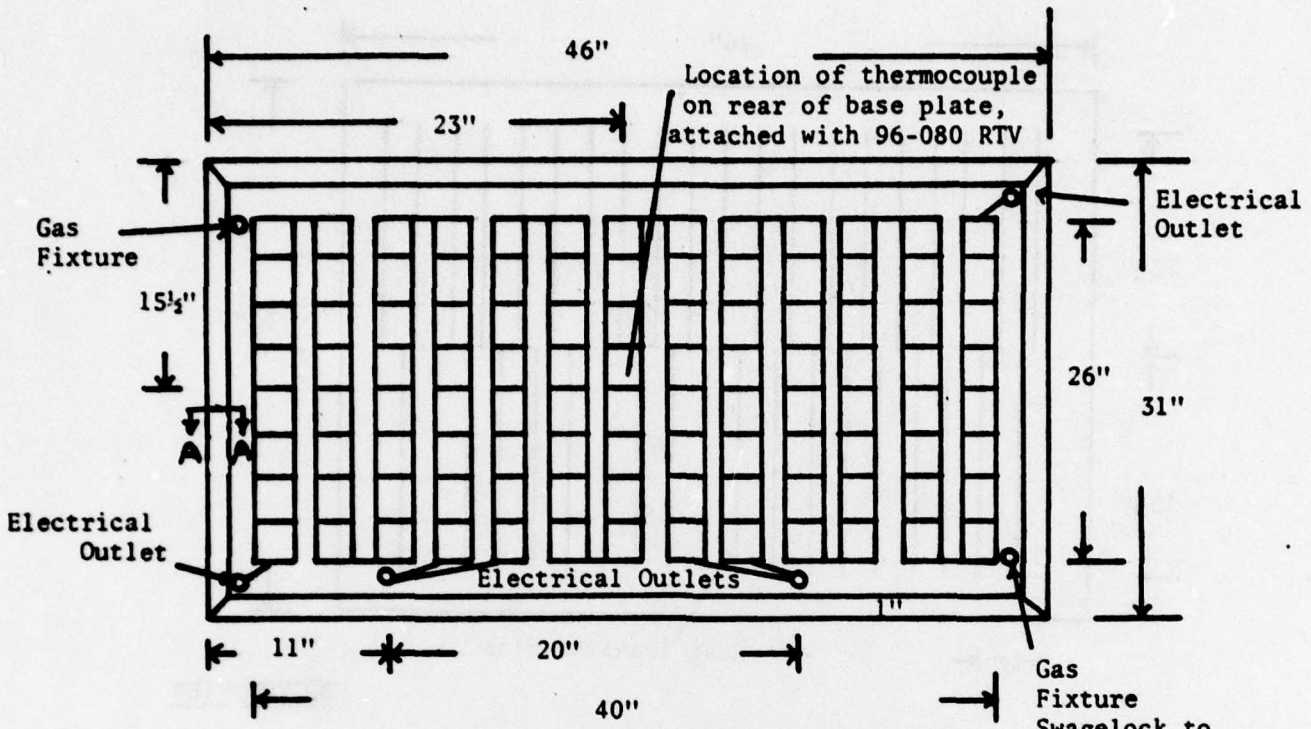

DETAIL OF CROSS SECTION A-A FOR VARIOUS SUBPANELS

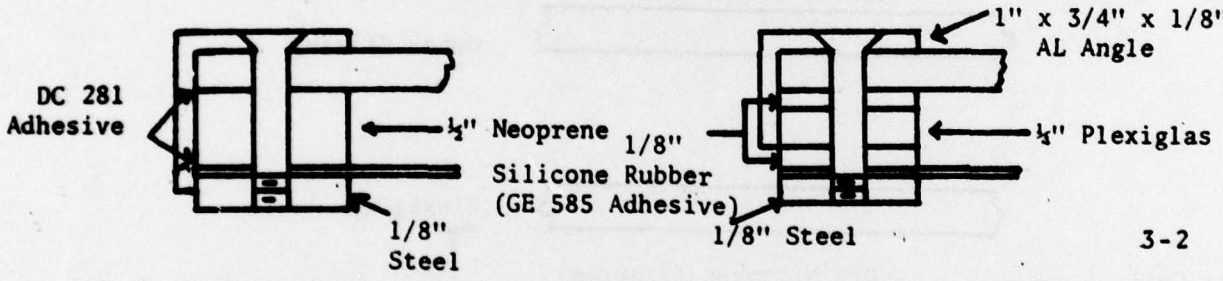

1-2, 1-1, 1-3

3-2

10-32 FHMS (Used in All Four Designs

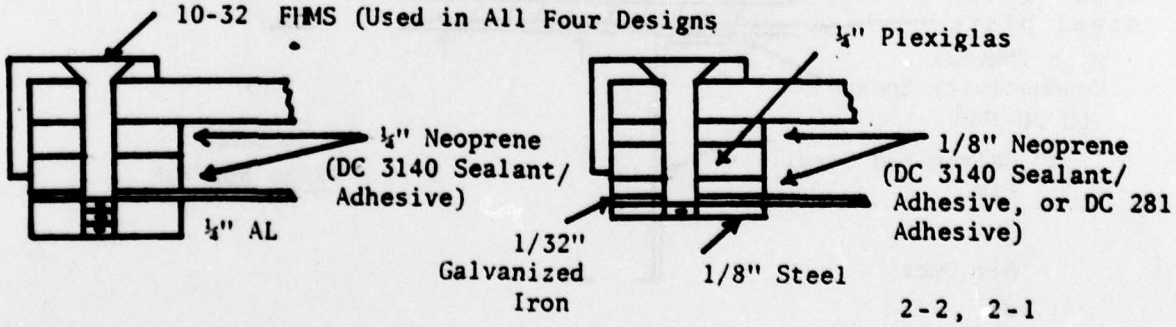

2-3

2-2, 2-1

FIGURE 4 (continued)

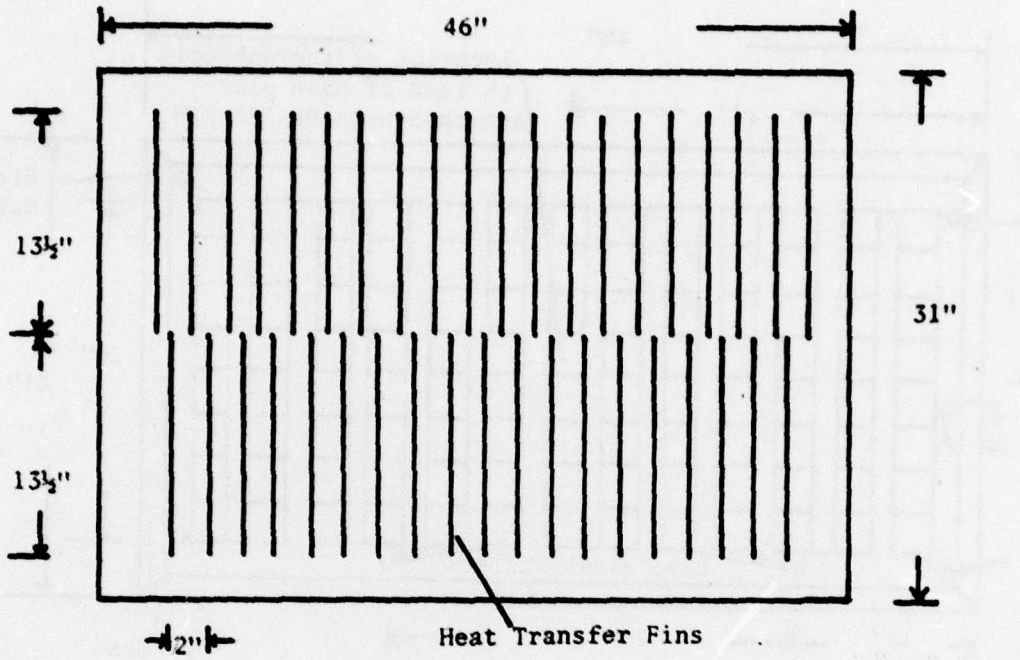

BOTTOM VIEW

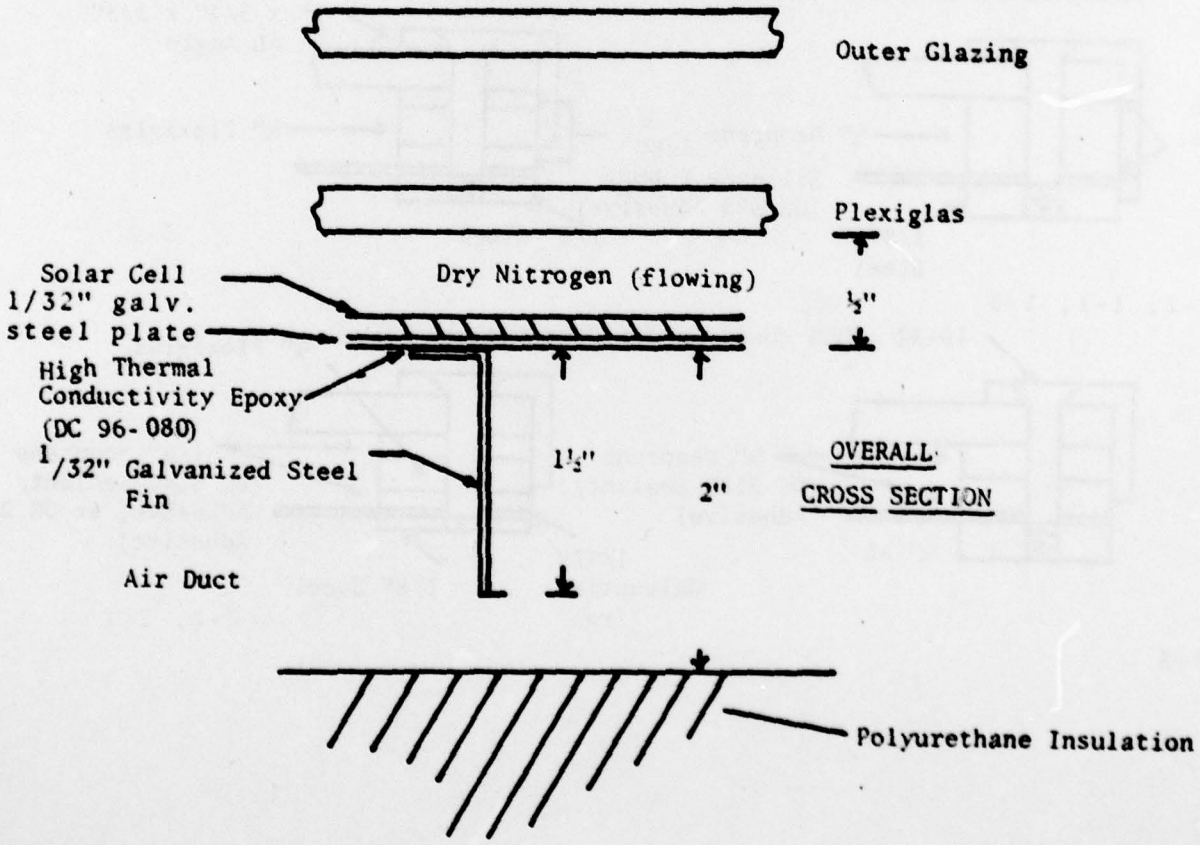

FIGURE 5

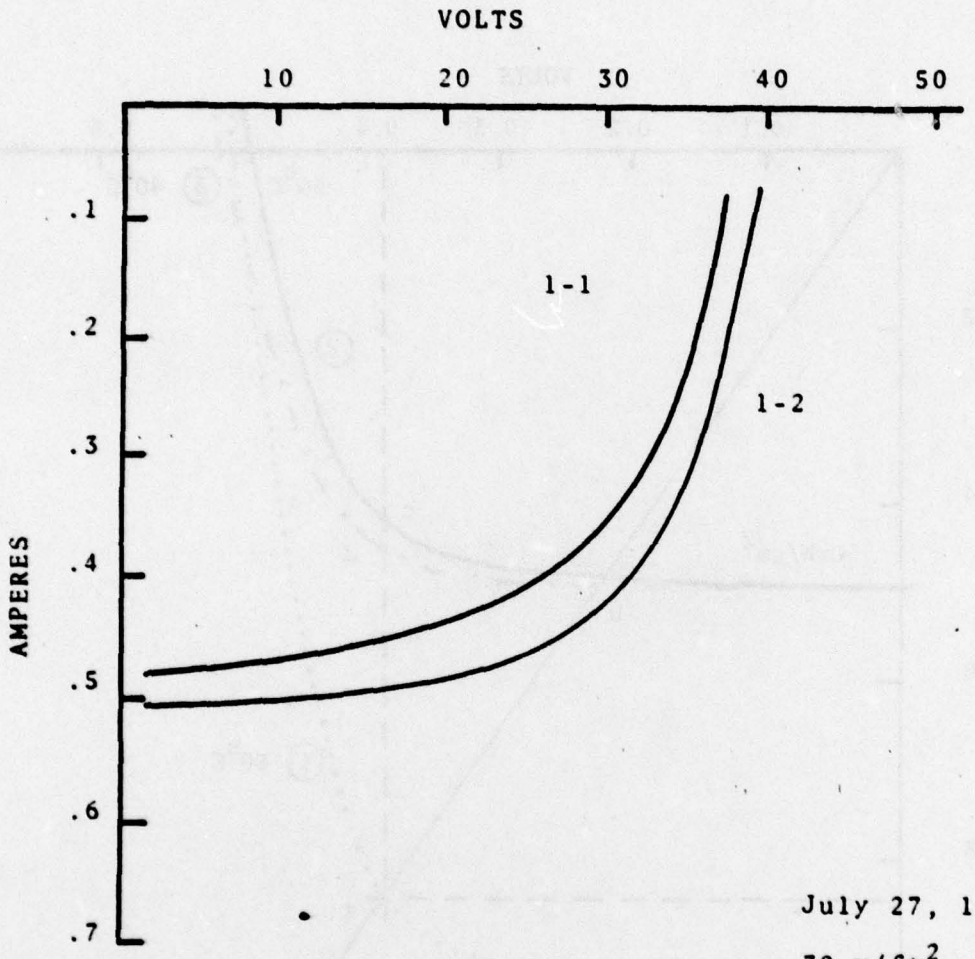

July 27, 1973

79 w/ft^2

FIGURE 6

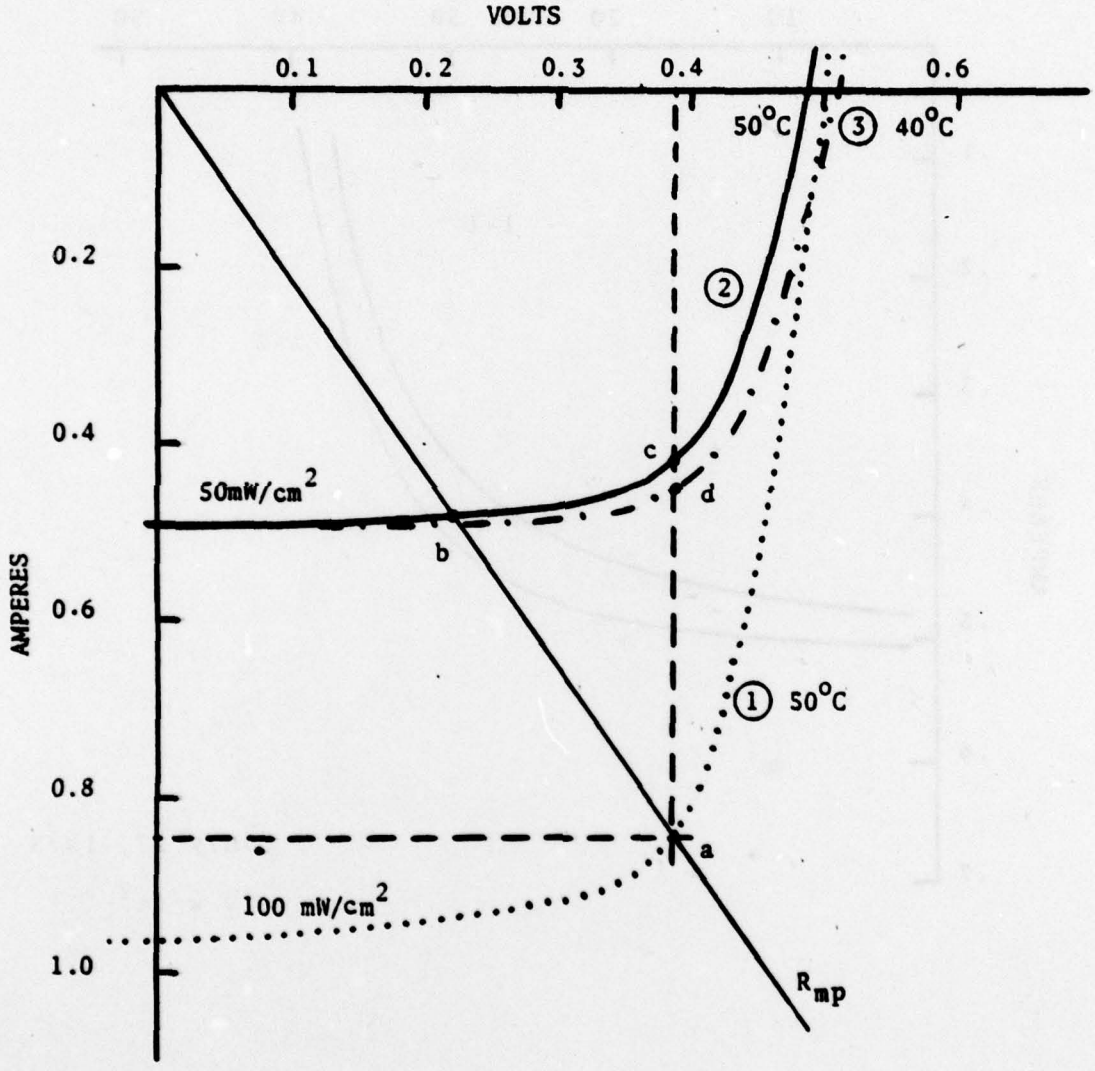
VOLTS
0.1
0.2
0.3
0.4
0.6
50°C
3
40°C
0.2
2
0.4
c
50mW/cm²
d
b
AMPERES
0.6
1
50°C
0.8
a
100 mW/cm²
1.0
Rmp

FIGURE 7

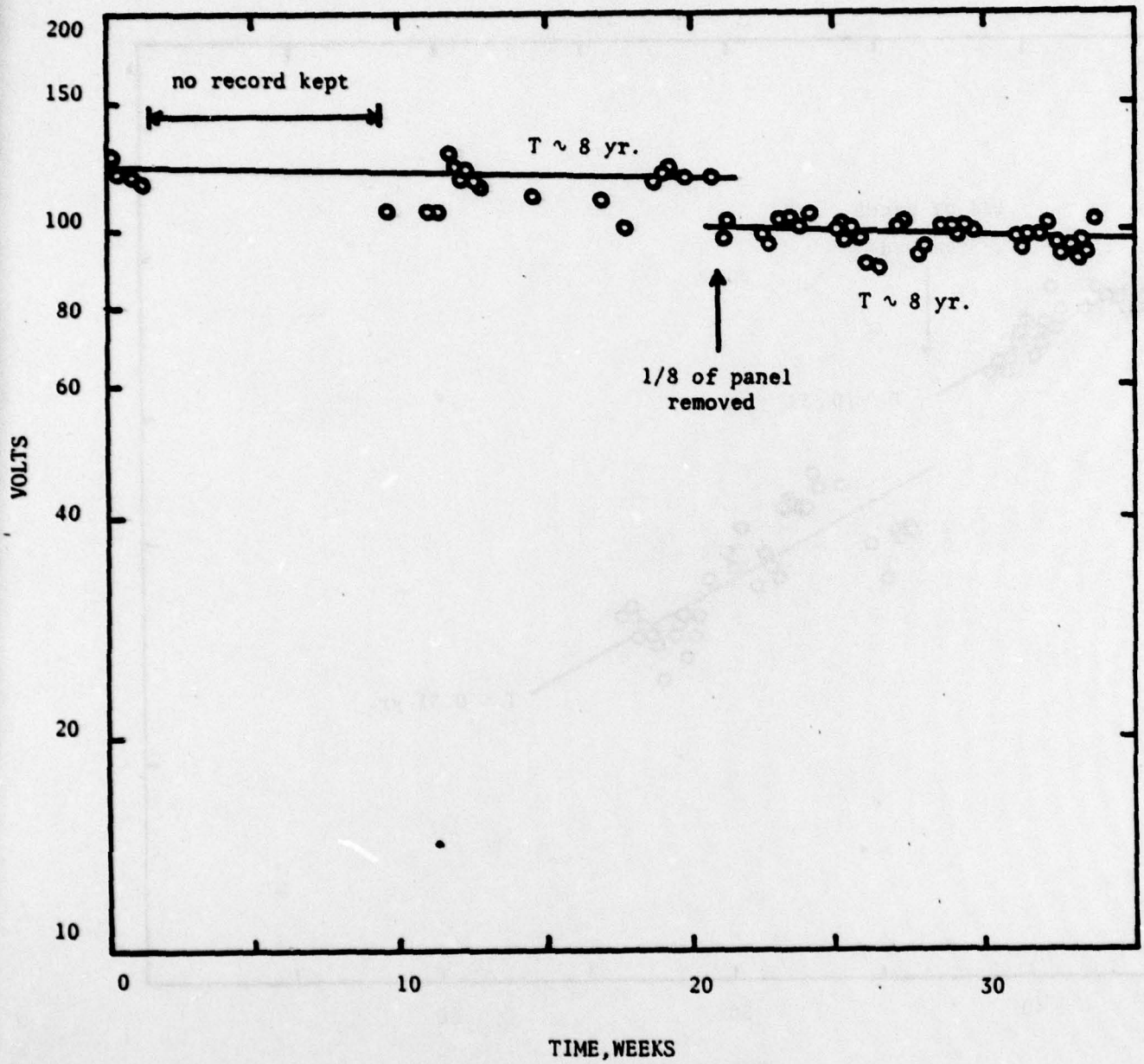
200
150
100
80
60
40
20
10
VOLTS
no record kept
T ∿ 8 yr.
T ∿ 8 yr.
1/8 of panel
removed
0
10
20
30
TIME, WEEKS

FIGURE 8

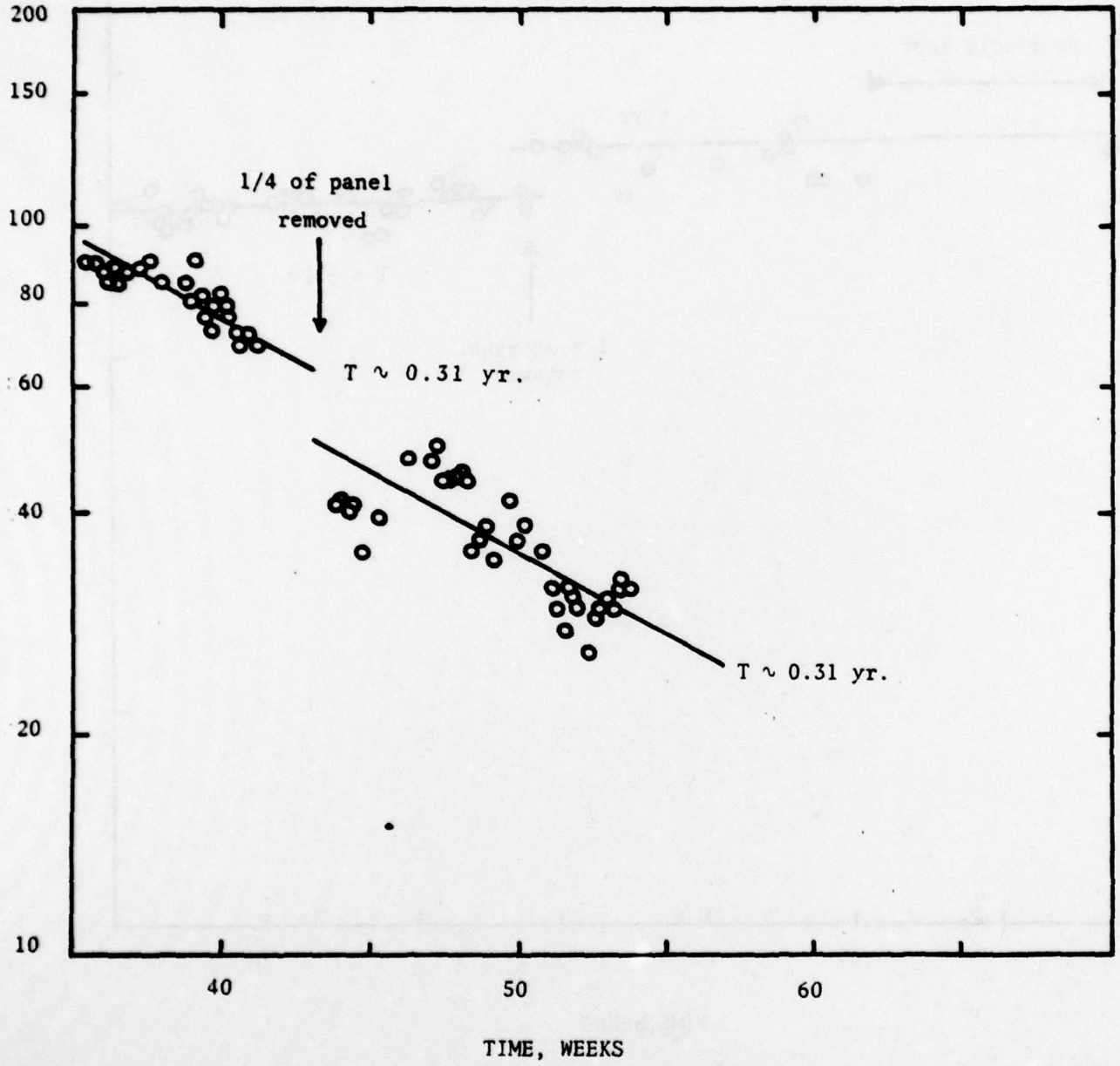
200
150
100
80
60
40
20
10
VOLTS
1/4 of panel
removed
T ∿ 0.31 yr.
T ∿ 0.31 yr.
40
50
60
TIME, WEEKS

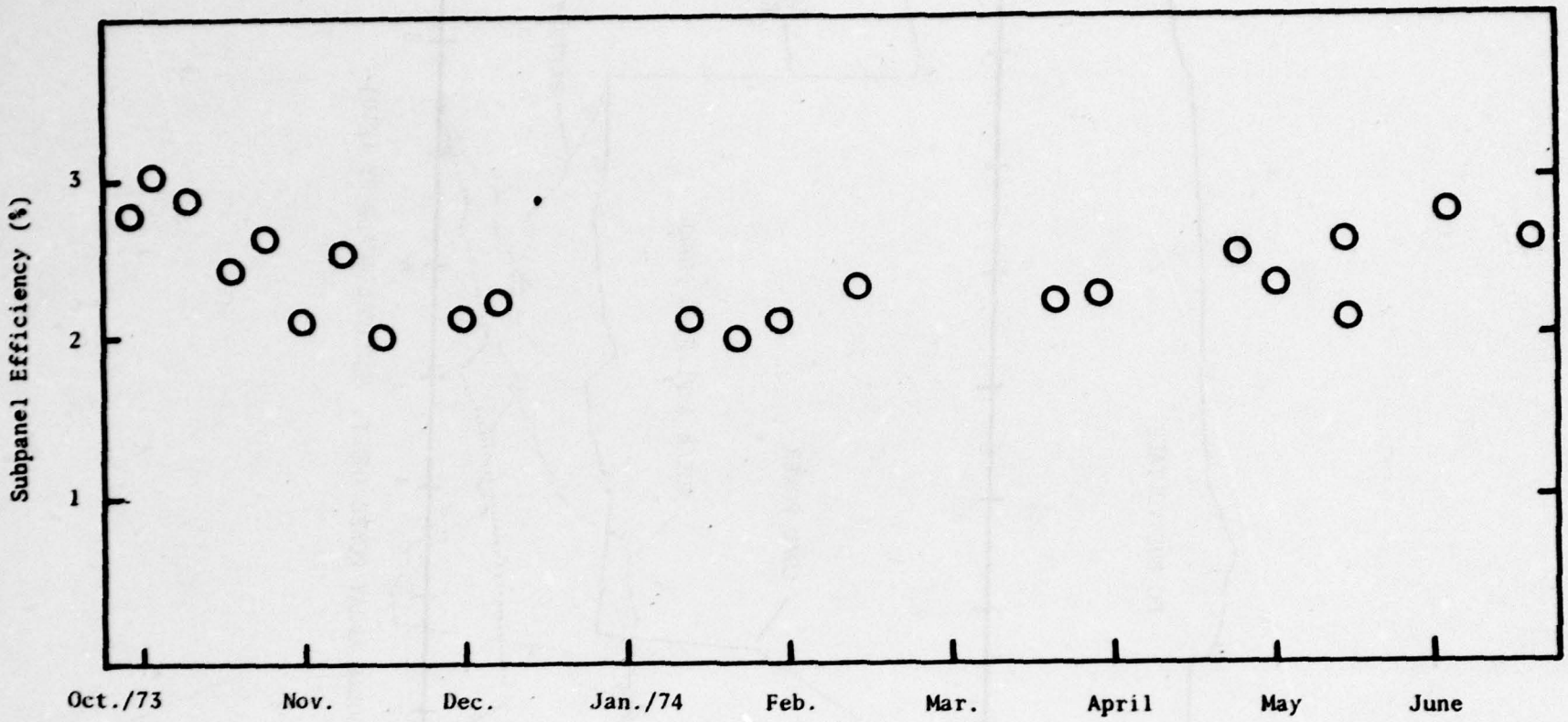
Subpanel Efficiency (%)
3
2
1
Oct./73
Nov.
Dec.
Jan./74
Feb.
Mar.
April
May
June

FIGURE 9

FIGURE 10

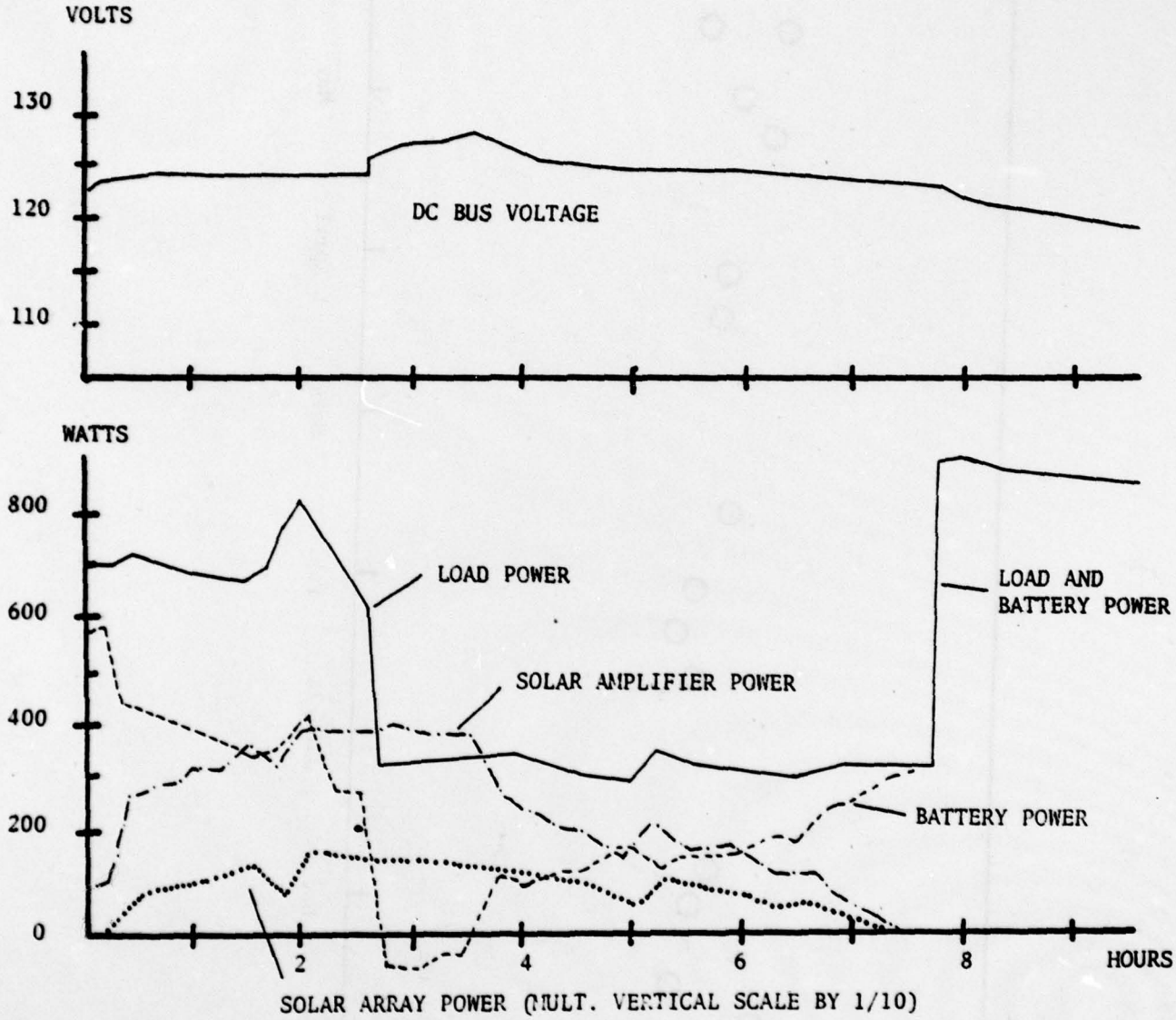
VOLTS
130
120
110
DC BUS VOLTAGE
WATTS
800
600
400
200
0
LOAD POWER
LOAD AND
BATTERY POWER
SOLAR AMPLIFIER POWER
BATTERY POWER
2
4
6
8
HOURS
SOLAR ARRAY POWER (MULT. VERTICAL SCALE BY 1/10)

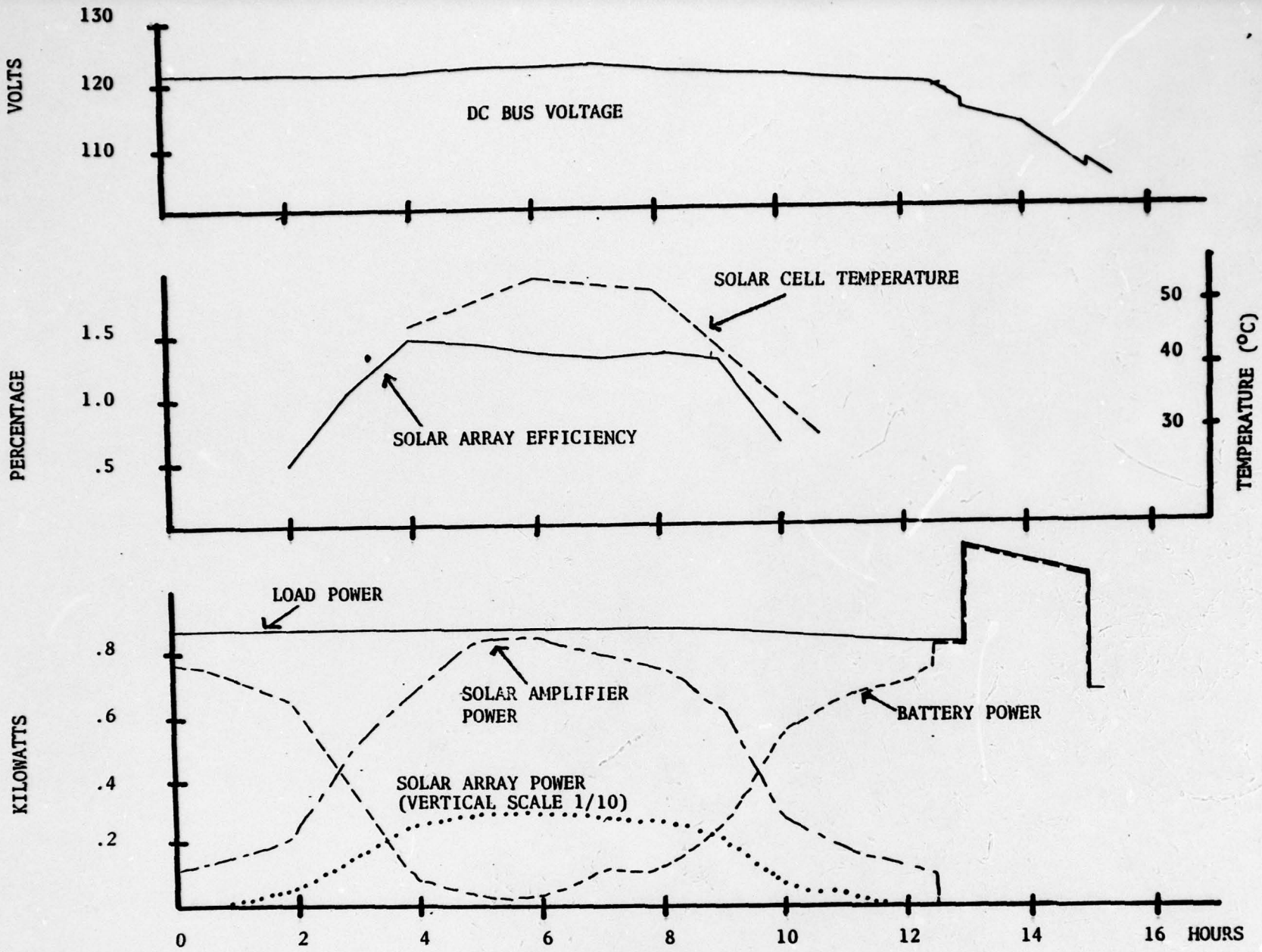
VOLTS
130
120
110
DC BUS VOLTAGE
PERCENTAGE
1.5
1.0
.5
SOLAR CELL TEMPERATURE
SOLAR ARRAY EFFICIENCY
50
40
30
TEMPERATURE (°C)
KILOWATTS
.8
.6
.4
.2
LOAD POWER
SOLAR AMPLIFIER POWER
BATTERY POWER
SOLAR ARRAY POWER (VERTICAL SCALE 1/10)
0
2
4
6
8
10
12
14
16
HOURS

FIGURE 11